Published OnlineFirst December 17, 2014; DOI: 10.1158/1535-7163.MCT-13-1084

Small Molecule Therapeutics

Molecular Cancer Therapeutics

The Use of Dipeptide Derivatives of 5-Aminolaevulinic Acid Promotes Their Entry to Tumor Cells and Improves Tumor Selectivity of Photodynamic Therapy

Gabriela Di Venosa[1], Pablo Vallecorsa[1], Francesca Giuntini[2], Leandro Mamone[1], Alcira Batlle[1], Silvia Vanzuli[3], Angeles Juarranz[4], Alexander J. MacRobert[5], Ian M. Eggleston[2], and Adriana Casas[1]

Abstract

The use of endogenous protoporphyrin IX generated after administration of 5-aminolaevulinic acid (ALA) has led to many applications in photodynamic therapy (PDT). However, the bioavailability of ALA is limited by its hydrophilic properties and limited cell uptake. A promising approach to optimize the efficacy of ALA-PDT is to deliver ALA in the form of prodrugs to mask its hydrophilic nature. The aim of this work was to evaluate the potential of two ALA dipeptide derivatives, N-acetyl terminated leucinyl-ALA methyl ester (Ac-Leu-ALA-Me) and phenylalanyl-ALA methyl ester (Ac-Phe-ALA-Me), for their use in PDT of cancer, by investigating the generation of protoporphyrin IX in an oncogenic cell line (PAM212-Ras), and in a subcutaneous tumor model. In our *in vitro* studies, both derivatives were more effective than ALA in PDT treatment, at inducing the same protoporphyrin IX levels but at 50- to 100-fold lower concentrations, with the phenylalanyl derivative being the most effective. The efficient release of ALA from Ac-Phe-ALA-Me appears to be consistent with the reported substrate and inhibitor preferences of acylpeptide hydrolase. *In vivo* studies revealed that topical application of the peptide prodrug Ac-Phe-ALA-Me gave greater selectivity than with ALA itself, and induced tumor photodamage, whereas systemic administration improved ALA-induced porphyrin generation in terms of equivalent doses administered, without induction of toxic effects. Our data support the possibility of using particularly Ac-Phe-ALA-Me both for topical treatment of basal cell carcinomas and for systemic administration. Further chemical fine-tuning of this prodrug template should yield additional compounds for enhanced ALA-PDT with potential for translation to the clinic. *Mol Cancer Ther; 14(2); 440–51. ©2014 AACR.*

Introduction

Photodynamic therapy (PDT) is a nonthermal technique for inducing tissue damage with light following administration of a light-activated photosensitizing drug that can be selectively retained in malignant or diseased lesions relative to normal adjacent tissue (1–3). In recent years, 5-aminolaevulinic acid (ALA)-mediated PDT has become one of the most promising fields in PDT research. ALA is the prodrug of the photosensitizer protoporphyrin IX (PpIX). After ALA administration, cells generate PpIX through the heme biosynthetic pathway. Clinically, when sufficient intracellular levels of PpIX are attained following either topical or oral ALA administration, the targeted tissue is irradiated with visible light to activate the sensitizer, leading to the generation of cytotoxic species and ultimately cell death. At a molecular level, this involves the interaction of the excited photosensitizer with molecular oxygen, leading to the generation of electrophilic species (singlet oxygen and/or radicals) that cause oxidative damage to cellular constituents such as phospholipidic membranes, nucleic acids, and proteins (4).

The main advantage of ALA-induced PpIX relative to other photosensitizers is the short half-life of its photosensitizing effects, which do not last longer than 48 hours (5). Moreover, ALA also has great potential as a photodiagnostic or photodetection agent in clinical practice. The use of ALA-induced PpIX fluorescence is currently being exploited for diagnosis of bladder cancer, and intraepithelial lesions of the cervix, lung, and brain cancer (6–10). Although ALA-PDT has already shown great potential both for the treatment of cancer and infectious diseases (11, 12), its efficacy is somewhat limited by the hydrophilic nature of the molecule, leading to poor penetration through certain malignant tissues. At physiologic pH, ALA is a zwitterion, which severely impairs its ability to cross cell membranes via passive uptake, and may result in poor penetration and nonhomogeneous distribution in target tissues (13). In addition, saturation of

[1]Centro de Investigaciones sobre Porfirinas y Porfirias (CIPYP), CONICET and Hospital de Clínicas José de San Martín, University of Buenos Aires, Ciudad de Buenos Aires, Argentina. [2]Department of Pharmacy and Pharmacology, University of Bath, Bath, United Kingdom. [3]Instituto de Estudios Oncologicos, Academia Nacional de Medicina, Buenos Aires, Argentina. [4]Departamento de Biología, Facultad de Ciencias, Universidad Autónoma de Madrid, Cantoblanco, Madrid, Spain. [5]Division of Surgery and Interventional Sciences and UCL Institute of Biomedical Engineering, University College London, London, United Kingdom.

Corresponding Author: Alexander J. MacRobert, Division of Surgery and Interventional Sciences and UCL Institute of Biomedical Engineering, University College London, Charles Bell House, 67-73 Riding House St, London W1W 7EJ, United Kingdom. Phone: 442076799384; Fax: 442078132828; E-mail: a.macrobert@ucl.ac.uk

doi: 10.1158/1535-7163.MCT-13-1084

Published OnlineFirst December 17, 2014; DOI: 10.1158/1535-7163.MCT-13-1084

heme synthesis as well as photobleaching of PpIX are also factors limiting the outcome of ALA-PDT (14, 15). To address these issues, a variety of ALA prodrugs have been investigated, incorporating specific chemical modifications that may provide enhanced uptake and hence higher PpIX production and thus photosensitization (16). The conversion of ALA to ester prodrugs with enhanced lipophilicity has been extensively investigated, and various studies have demonstrated that esterification of ALA with both aliphatic linear and cyclic alcohols reduces the amount of ALA required for photosensitization (17–21). Prodrugs of this kind, in particular methyl (Me-ALA) and hexyl ester (He-ALA) derivatives of ALA, have now been validated in a clinical setting, with regulatory approval being granted for the use of Me-ALA for the treatment of actinic keratosis in Europe and the United States (22, 23), and basal cell carcinoma in Europe (23). He-ALA has also been approved in Europe for its use in fluorescence cystoscopy (24).

Other chemical approaches to enhance ALA-PDT have focused on increasing the payload of ALA that may be delivered by a single prodrug entity, as well as combining ALA administration with the use of other molecules that may boost PpIX production, by blocking downstream ferrochelatase-catalyzed conversion of PpIX to heme. In the latter case, various iron chelators (25–28) and chemotherapeutic agents (29) have been shown to be effective in enhancing levels of PpIX production upon administration of ALA. The use of ALA conjugated to first- or second-generation dendrimers also results in enhanced porphyrin synthesis with such prodrugs at low concentrations compared with an equivalent dose of ALA itself (30–33).

An attractive way to obtain ALA prodrugs that have both improved physicochemical properties and can selectively release ALA in specific cell lines is to incorporate ALA into a short peptide derivative (34–37).

Upon cellular uptake, ALA release may be mediated by the action of cytoplasmic esterases and/or proteases. Following this approach, Giuntini and colleagues (38) synthesized a range of ALA dipeptide derivatives that are uncharged at physiologic pH, and are more lipophilic than ALA, yet retain adequate aqueous solubility. They are also stable at physiologic pH, unlike ALA and its esters. The general structure of these compounds is shown in Fig. 1, and they were demonstrated to be incorporated into the immortalized PAM212 cell line with significantly greater efficiency than ALA itself. Significantly, the efficiency of uptake of any given prodrug was not directly correlated with downstream PpIX production, showing that ALA release was mediated by a specific protease activity. Indeed, prodrugs containing a D-amino acid component are incorporated but not processed, whereas in cell lines such as A549 epithelial carcinoma that have a low expression of acyl-peptide hydrolase (a protease shown to release ALA from these compounds; ref. 39), efficient prodrug uptake, but low ALA release and PpIX production were observed. These encouraging *in vitro* results and studies in skin explant models (40) highlight the possibility to design peptide prodrugs of this type that can be used to target disease-specific levels of a given enzymatic activity to provide selective ALA release. In this context, it is important to evaluate the most promising of these prototypes in clinically relevant cancer cell lines and *in vivo* to assess the real potential of this novel strategy for ALA-PDT.

The aim of the present work was to investigate *in vivo* the properties of two ALA dipeptide prodrugs, N-acetyl terminated leucinyl (Ac-Leu-ALA-Me) and phenylalanyl-ALA (Ac-Phe-ALA-Me), which have previously been shown to exhibit significantly enhanced cellular uptake and PpIX-induced phototoxicity compared with ALA. We used the keratinocyte normal/tumor cell line pair PAM212 and PAM212-Ras as an *in vitro* model, and the mammary carcinoma cell line LM2 as an *in vivo* model of a subcutaneous transplantable tumor.

Materials and Methods

Chemicals

ALA-HCl and MTT were from Sigma Chem Co. Ac-Leu-ALA-Me and Ac-Phe-ALA-Me, were synthesized according to the method described by Rogers and colleagues (37) and Giuntini and colleagues (38). Stock solutions were prepared by dissolving at 10 mmol/L in 0.01 mol/L HCl and buffered with 0.01 mol/L NaOH before use. He-ALA was synthesized according to the method of Takeya (41) by reacting ALA with hexanol in the

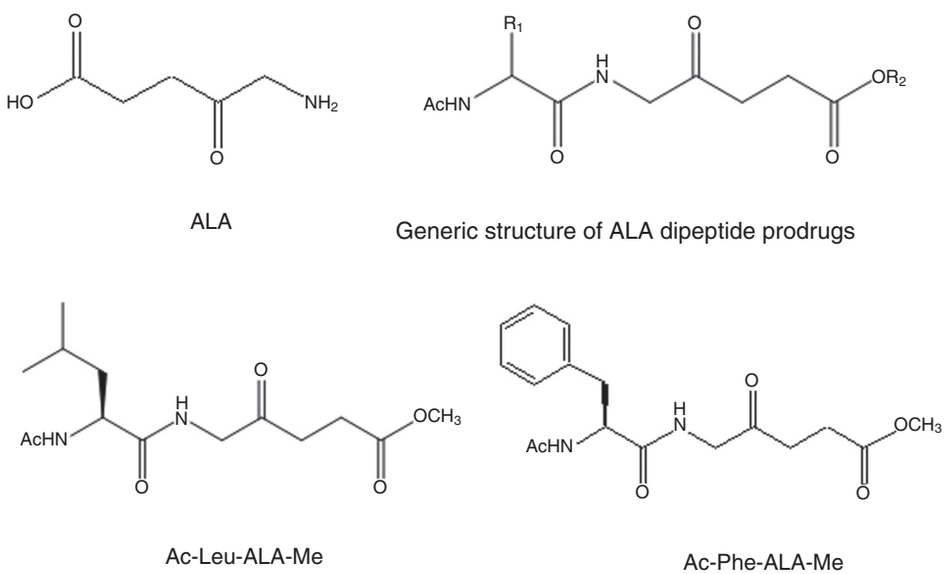

Figure 1.
Structures of ALA and Ac-Leu-ALA-Me and Ac-Phe-ALA-Me dipeptides.

Published OnlineFirst December 17, 2014; DOI: 10.1158/1535-7163.MCT-13-1084

presence of thionyl chloride. The mixture was stirred at 70°C until ALA-HCl was completely dissolved and the reaction was confirmed by TLC (CH_2Cl_2:MeOH 9:1). The excess alcohol was evaporated off under high vacuum. After the addition of diethyl ether, the HCl salt of the ALA ester was allowed to crystallize at 4°C.

Cell lines

PAM212 is an immortalized and spontaneously transformed cell line from a BALB/c primary keratinocyte culture (42). These cell lines were previously characterized genetically and morphologically, and have not been retested and authenticated in the present study. Retroviruses encoding oncogenic $HRAS^{(V12)}$ with a neomycin resistance marker were produced and stably transfected into PAM212 cells as previously described (43). Controls for *HRAS* presence were periodically carried out by Western blot assays. Cell lines were passaged three times when first obtained, and then frozen and stored at −80°C or in liquid nitrogen to provide low-passage cells to renew the stock as required. Our policy was to reestablish the line from frozen stock after a maximum of 20 weeks in culture. After cultivation in 400 μg/mL G418 (Calbiochem, Merck) for 7 days, transfected cells were routinely grown in RPMI-1640 medium (Gibco BRL, Life Technologies Lt) containing L-glutamine 2 mmol/L and phenol red, supplemented with 10% FCS and incubated at 37°C in an atmosphere containing 5% CO_2. Cells were used 48 hours after plating.

PDT treatment

Cells were incubated in serum-free medium containing ALA or peptides and 3 hours later, irradiations were performed. After irradiation, medium was replaced by ALA-free medium + serum, the cells were incubated for another 19 hours and then tested for viability. Median lethal light doses (LD50) were calculated as mJ/cm^2, leading to 50% of cell viability.

MTT viability assay

Phototoxicity and cell viability were determined by the MTT assay (44), which is based on the activity of mitochondrial dehydrogenases. Following treatment, MTT (3-[4,5-dimethylthiazol-2-yl]-2,5-diphenyl-tetrazoliumbromide) solution was added to each well in a concentration of 0.5 mg/mL, and plates were incubated at 37°C for 1 hour. The resulting formazan crystals were dissolved by the addition of DMSO and the absorbance was read at 560 nm.

Light source

A bank of two fluorescent lamps (Osram L 18W/765) was used. The spectrum of light was between 400 nm and 700 nm with the highest radiant power at 600 nm. The plates were located at a distance of 14 cm from the light source, and the cells were irradiated from below. The fluence rate was measured with a radiometer (model 65, Yellow Springs). We used fluences between 10 mJ/cm^2 and 150 mJ/cm^2 and power density was 0.5 mW/cm^2

Porphyrin extraction from cells

Porphyrins accumulated within the cells were extracted twice with 5% HCl, leaving the cells standing for 30 minutes in the presence of the acid at 37°C. These conditions proved to be optimal for total PpIX extraction. For media determinations, 5% HCl was added and the fluorescence was measured directly. The fluorescence was determined using a fluorescence spectrometer (PerkinElmer LS50B, excitation and emission wavelengths were 406 nm and 604 nm, respectively). PpIX (Frontier Sciences) was used as a reference standard.

Animals

Male BALB/c mice 12 weeks old, weighing 20 to 25 g were used. They were obtained from the School of Sciences, University of Buenos Aires, and provided with food (Purina 3, Molinos Río de la Plata, Argentina) and water *ad libitum*. A suspension of 1.6×10^5 cells of the LM3 cell line was subcutaneously injected on the flanks of the mice. Experiments were performed at approximately day 20 after implantation. Tumors of the same uniform size were used (1 cm diameter). Animals received human care and protocols were approved by the Argentinean Committee (CICUAL, School of Medicine, University of Buenos Aires) in full accordance with the UK Guidelines for the Welfare of animals in Experimental Neoplasia (45).

ALA and ALA dipeptide administration

ALA was dissolved in saline to a final volume of 0.15 mL immediately before intraperitoneal (i.p.) injection. For topical administration, ALA was dissolved in 0.2 mL saline immediately before use, whereas ALA-dipeptides were dissolved in HCl, then equimolar NaOH was titrated until pH 7 and the volume was completed with saline. ALA formulations were applied on the skin overlying the tumor (SOT), after shaving the hair and rubbing with a smooth paintbrush for a period of 5 minutes, a time at which no vestiges of lotion were visible. Two areas of skin were investigated: SOT and normal skin taken from the opposite flank, denoted as "distant skin."

Porphyrin extraction from tissues

After ALA or ALA derivatives i.p. injections, animals were sacrificed. Before killing, mice were injected with heparin (0.15 mL, 1,000 UI), and after sacrifice, they were perfused with 200 mL of sterile saline. The organ samples were homogenized in a 4:1 solution of ethyl acetate:glacial acetic acid. The mixtures were centrifuged for 30 minutes at 3,000 g, and the supernatants were diluted with an equal volume of 5% HCl. Extraction with HCl was repeated until there was no detectable fluorescence in the organic layer. The aqueous fraction was used for the measurement of porphyrins. The fluorescence was determined using a PerkinElmer LS50B fluorescence spectrometer, excitation and emission wavelengths were 406 nm and 604 nm, respectively), using PpIX as the reference standard.

Fluorescence spectroscopy

In vivo fluorescence measurements were carried out to investigate the kinetics of PpIX formation after topical application of ALA or ALA dipeptides. A bifurcated fiber-optic probe was coupled to a PerkinElmer LS50B fluorescence spectrometer, and fluorescence from the tissue was detected at the probe tip. Excitation light at a wavelength of 407 nm was coupled into one arm of the birfurcated probe, enabling conduction of excitation to the skin surface and collection of the PpIX fluorescence emission via the other arm to the spectrometer. Taking into account the attenuation coefficient for skin, the 407-nm light penetrates deep enough into the skin to excite the PpIX in the epidermis and dermis (46). The fiber tip was fitted with a rubber spacer that ensured a constant fixed distance of 7 mm between the fiber and the tissue and provided optimal signal collection from the tissue. Fluorescence intensity

Published OnlineFirst December 17, 2014; DOI: 10.1158/1535-7163.MCT-13-1084

was measured as a function of time and expressed in arbitrary units at an emission wavelength of 635 nm. In addition, fluorescence emission spectra were measured to verify that the fluorescence signal corresponded to PpIX.

Fluorescence imaging of PpIX biodistribution following topical application of ALA and Ac-Phe-ALA-Me

For recording of fluorescence micrographs of SOT + tumor, samples were frozen and 15-μm thick cryosections were prepared. Both samples and sections were always handled under subdued lighting conditions. Microscopic observation was performed (Olympus BX51 microscope) using excitation at 545 nm using a bandpass filter and images were recorded using a Q-color 5 camera. After fluorescence observation, sections were stained with hematoxylin and eosin to identify fluorescence localization.

PDT procedure and histologic studies

ALA and ALA peptides at dose equivalents of 3 mg were applied topically on the SOT of tumor-bearing mice, 3 hours before irradiation. Subsequently, animals were anesthetized by i.p. injection of 70 mg/kg ketamine hydrochloride and 6 mg/kg xylazine and tumors were superficially irradiated. During illumination, normal tissue surrounding the tumor was shielded with a piece of black plastic, leaving exposed a peritumoral margin of 3 mm.

For tumor illumination, a diode InGaAsP 635 nm laser (Lumiia AccuraBeam) was used. The light was focused into a 400-mm diameter optical fiber and the cut end of the fiber was positioned to provide a 1.5-cm diameter light spot, producing a treatment area of uniform intensity. The output power from the fiber was measured with a power meter (Fieldmaster LM-100XL with a LM3HTD sensor, Coherent). Total doses of 96 J/cm^2 were delivered using a fluence rate of 80 mW/cm^2 over 20 minutes. These light doses do not cause additional hyperthermic effects, which may influence the efficacy of PDT.

One day after PDT, mice were sacrificed and samples of tumors with their adjacent SOTs were excised, extended, sliced, fixed in 10% buffered formalin, embedded in paraffin, sectioned, stained with hematoxylin and eosin, and examined by light microscopy under ×10 and ×40 magnifications using a BX51 Olympus microscope, and photographs were documented with a Q-color 5 camera.

Statistical analysis

The values in the figures and tables are expressed as mean ± SDs of the mean. A two-tailed Student *t* test was used to determine statistical significance between means. To compare PDT responses between PAM212 and PAM212-Ras cells for each prophotosensitizer, LD50s were calculated from the light dose–response curves using using a three parameter logistic equation (GraphPad Prism). LD50 values were calculated as the geometric mean ± 95% confidence intervals of the log-transformed curves. Statistical comparisons between LDs were made using the Student *t* test, and the null hypothesis rejected when $P < 0.05$.

Results

We evaluated porphyrin synthesis from ALA and its derivatives in PAM212 and PAM212-Ras cell lines (Fig. 2). After a 3-hour incubation period, the highest porphyrin levels using the lowest concentration (6.1 ± 0.2 and 6.6 ± 0.5 ng porphyrins/10^5 cells for PAM212 and PAM212-Ras, respectively) were obtained from Ac-Phe-ALA-Me at 0.01 mmol/L concentrations. The amount of porphyrins obtained from Ac-Leu-ALA-Me (4.8 ± 0.4 and 6.0 ± 0.4 ng porphyrins/10^5 cells for PAM212 and PAM212-Ras, respectively) at 0.01 mmol/L were also higher than those obtained from ALA (2.3 ± 0.2 and 2.6 ± 0.2 ng porphyrins/10^5 cells), which were comparable with the basal porphyrin values. The most efficient porphyrin synthesis was observed with Ac-Phe-ALA-Me, which was even better than the well-known ALA ester He-ALA, inducing 4.9 ± 0.3 and 5.7 ± 0.6 ng porphyrins/10^5 PAM212 and PAM212-Ras cells, respectively, at 0.01 mmol/L concentration.

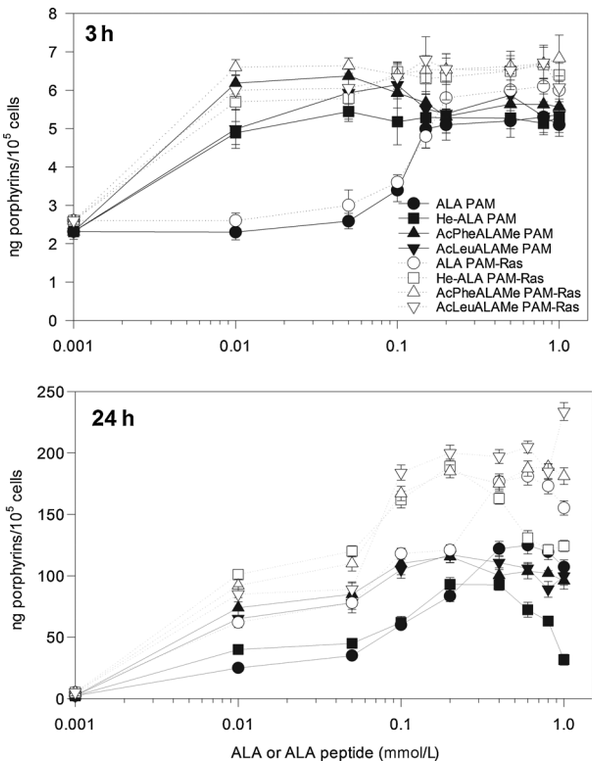

Figure 2.
Porphyrin synthesis from ALA or ALA derivatives in PAM212 and PAM212-Ras cells. Cells were exposed to different concentrations of ALA or ALA derivatives during 3 or 24 hours. Intracellular porphyrin levels were determined fluorometrically and normalized per number of cells present at the end of the experiment.

Plateau values are obtained from the ALA peptides in the 0.01 to 0.05 mmol/L range, whereas from He-ALA, they are obtained at 0.05 and 0.5 mmol/L from ALA.

Overall, PAM212-Ras porphyrin values are higher than those observed using PAM212, for all concentration ranges and irrespective of the compound used.

By using longer incubation periods of 24 hours, the profiles of porphyrins synthesis are similar to the 3-hour ones. With either ALA or ALA derivatives, the amount of tetrapyrroles formed from the RAS-transfected cell line is still significantly higher as compared with the parental cell line. Plateau values are obtained for all the prodrugs and both cell lines, at higher concentrations as compared with 3-hour incubation, due to substrate consumption.

In line with the patterns of porphyrin synthesis, Fig. 3 shows that the higher the amount of porphyrins, the higher the

Published OnlineFirst December 17, 2014; DOI: 10.1158/1535-7163.MCT-13-1084

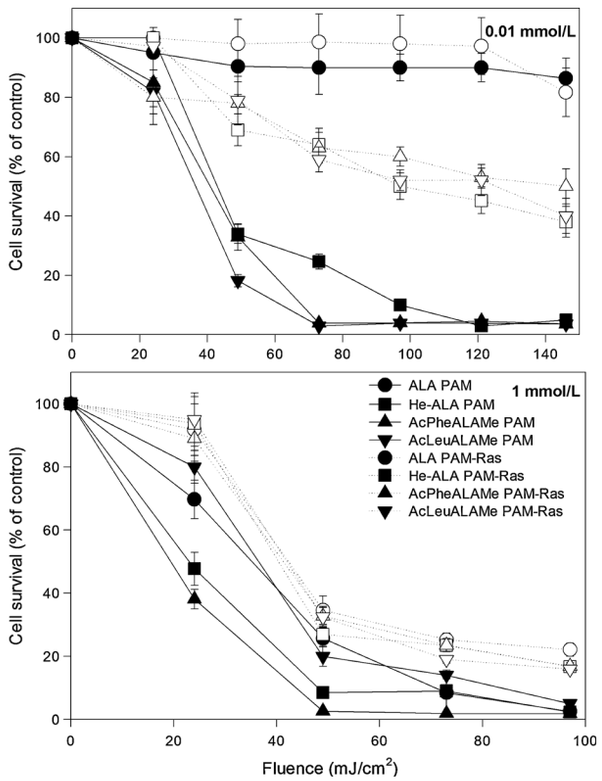

Figure 3.
Cell survival after PDT. Cells were incubated with 0.01 or 1 mmol/L ALA or ALA derivatives during 3 hours. Afterward, PDT was performed, and cell viability was evaluated by the MTT assay, as percentage of control nonirradiated cells.

photocytotoxicity for a given dose comparing the four compounds within the same cell line. Overall, PAM212-Ras cells are more resistant to PDT despite synthesizing higher amounts of porphyrins.

PDT was applied after 3-hour incubation of prodrugs at 0.01 mmol/L, which is a plateau concentration for ALA derivatives but not for ALA. At this concentration, phototoxicity from ALA is almost negligible, whereas from all ALA derivatives, the LD50s were around 135 mJ/cm^2 for PAM212-Ras cells, and 45 mJ/cm^2 for PAM12 cells. Under these conditions, comparing the corresponding LD50s for each prophotosensitizer, PAM212-Ras cells were significantly less responsive to ALA derivatives PDT treatments as compared with the parental line.

Using a plateau concentration for both ALA and derivatives (1 mmol/L), LD50s are about 45 mJ/cm^2 for PAM212-Ras and in the range of 20 to 30 mJ/cm^2 for PAM212 cells These LD values are still significantly higher in Ras-transfected cells for Ac-Phe-ALA-Me and He-ALA, but not significantly different for ALA and the Ac-Leu-ALA-Me derivative.

By means of fiber-optic fluorescence detection, we analyzed porphyrin formation as a function of time after topical application of ALA and ALA dipeptides on the SOT of implanted mice (Fig. 4). ALA induces similar profiles of porphyrin production in SOT as compared with distant skin, this being a consequence of rapid diffusion of the molecule to other sites, immediately after application. On the other hand, although Ac-Phe-ALA-Me induced lower amounts of porphyrins in both skin types as compared with ALA, selectivity for SOT is statistically improved at all time points (all, $P < 0.05$, Student t test). The ratio between SOT and distant normal skins is about 1.45 for the phenylalanyl dipeptide derivative, thus showing some confinement of the ALA peptide molecule to the site of application. On the other hand, Ac-Leu-ALA-Me is less efficient for porphyrin generation, producing in both skin types porphyrin levels which are four times lower than those obtained using ALA (differences between SOT and distant skins are not statistically significant). It is worth noting that in this system of superficial fluorescence detection, porphyrins confined to the most superficial layers of SOT invaded by tumor are mainly detected because blue light is used for excitation.

Table 1 describes the amount of porphyrins formed 3 hours after topical application of ALA and ALA peptides in tumor, SOT, and distant skin, quantified after chemical extraction of the different tissues at plateau times (see Fig. 4). Although both tumor and SOT porphyrins synthesized from ALA and Ac-Phe-ALA-Me are similar, distant skin values are significantly lower for the latter ($P = 0.046$), which represents a more selective tumor localization. On the other hand, the three tissues produce significantly lower porphyrins from Ac-Leu-ALA-Me as compared with ALA, without any increased selectivity.

Figure 5 describes the biodistribution of PpIX in SOT after topical application of ALA and Ac-Phe-ALA-Me. Although PpIX fluorescence from ALA is typically highest in the epidermis and hair follicles, its distribution from the phenylalanyl derivative appears to be less marked in the epidermis but strongly accumulated in hair follicles.

Figure 6 shows the hematoxylin and eosin-stained sections of control and ALA or Ac-Phe-ALA-Me topically treated subcutaneous tumors, illuminated, and excised 24 hours after treatment. The histologic response to PDT does not show large differences in

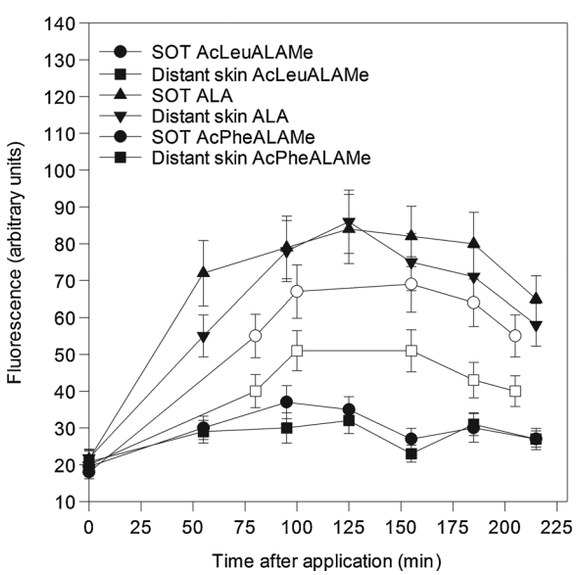

Figure 4.
Porphyrin synthesis in skin over the tumor and distant skin after topical application of ALA and ALA peptides. ALA and ALA peptides were applied topically to the SOT at dose equivalents of 3 mg ALA. At different times after application, the porphyrin fluorescence was monitored by a fiber optic probe coupled to a fluorescence spectrometer. Determinations were made on SOT and over a distant skin area. The average of three mice per treatment is shown.

Published OnlineFirst December 17, 2014; DOI: 10.1158/1535-7163.MCT-13-1084

Table 1. Porphyrin accumulation (μg porphyrin/g tissue) determined by chemical extraction in tumor, SOT, and a "distant" skin site after topical application on SOT of 3 mg ALA or dose equivalents of ALA dipeptides

	Tumor	SOT	Skin
ALA	0.21 ± 0.03	0.54 ± 0.09	0.44 ± 0.13
AcLeuALAMe	0.14 ± 0.01[a]	0.25 ± 0.03[a]	0.12 ± 0.04[a]
AcPheALAMe	0.21 ± 0.03	0.44 ± 0.09	0.22 ± 0.04[a]

[a]$P < 0.05$, compared with same tissue exposed to ALA.

the type or death distribution response between ALA and its derivative. The *stratum corneum* has partly or completely detached from the epidermis and pyknosis of epidermal cells is also observed, independent of the PpIX precursor used. Within the dermis, collagen fibers appear to be thickened and the presence of fibrosis and edema is evident.

The fat cells in the lower dermis are disorganized, and significant damage to hair follicles is observed, while the cutaneous musculature is preserved. The epidermis but not the dermis appears to be more preserved in the ALA peptide-treated SOT as compared with ALA.

Figure 7 shows the kinetics of porphyrin synthesis in a set of organs, after systemic application of Ac-Leu-ALA-Me and Ac-Phe-ALA-Me at dose equivalents of 120 mg/kg ALA.

In most tissues, porphyrin synthesis peaks at around 1 and 5 hours after ALA dipeptide administration. The liver is the only tissue that does not clear all the porphyrins synthesized from both molecules before 24 hours. In terms of maximal porphyrin accumulation, Ac-Phe-ALA-Me produces the highest values in all the tissues analyzed, around 20% higher than for Ac-Leu-ALA-Me. Although the kidney and intestine are the best porphyrins producers, the brain is the lowest. With respect to selectivity, neither of the ALA peptides gave rise to high porphyrin tumor levels relative to the skin or any other tissue.

Figure 8 shows a comparison of porphyrin synthesis in all tissues 3 hours after systemic administration of Ac-Leu-ALA-Me and Ac-Phe-ALA-Me at dose equivalents of 40 and 120 mg/kg of ALA. Ac-Phe-ALA-Me induces significantly more porphyrins in tumor as compared with ALA and the other peptide ($P = 0.0005$ and $P = 0.0006$) at 120 mg/kg, whereas in SOT and distant skin, the amount is similar as compared with ALA. The amount of tetrapyrroles induced by the leucinyl derivative is similar to ALA 120 mg/kg in tumor and skin but significantly lower in SOT ($P = 0.018$). As for the rest of tissues, the amount is similar for the three compounds.

Discussion

A relatively recent development in ALA-PDT concerns the preparation of peptide-based ALA prodrugs, and we (37, 38, 47) and others (35, 36) have described the synthesis and evaluation of short ALA peptide derivatives in which either the amino or the carboxyl functions of the latter are masked, thereby providing improved physical properties and the potential for cell line-specific ALA release, according to which peptidases are expressed.

The PAM212-Ras cell line synthesizes more porphyrins from ALA than its counterpart PAM212 cell line. However, it is more resistant to PDT, particularly when low prophotosensitizer concentrations are used. This feature has been previously observed by our group for the mammary cell line pair HB4a and HB4a-Ras (48), showing that overexpression of *RAS* oncogene confers resistance to ALA-PDT, independent of the amount of porphyrins synthesized. We were therefore intrigued to explore the effectiveness of prodrugs that are proven to perform significantly better than ALA in normal cell lines in this clinically relevant oncogenic system.

HRAS proteins play a direct causal role in human cancer and in other diseases. Mutant HRAS, NRAS, and KRAS occur with varying frequencies in different tumor types, for reasons that are unknown account for 20% to 30% of all human tumors (49, 50). Other members of the RAS superfamily may also contribute to cancer. Proteins in the RAS family are very important molecular switches for a wide variety of signal pathways that control processes such as cytoskeletal integrity, proliferation, cell adhesion, apoptosis, and cell migration.

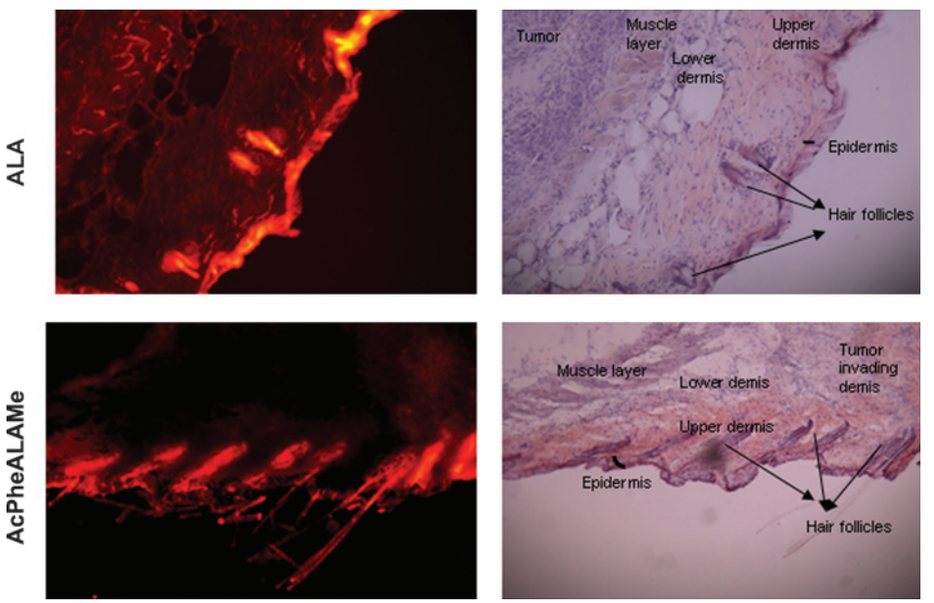

Figure 5.
Fluorescence images and hematoxylin and eosin-stained images of SOT and adjacent tumors topically applied with ALA and Ac-Phe-ALA-Me. ALA and ALA dipeptides were applied topically to the SOT at dose equivalents of 3 mg ALA, and animals were sacrificed 3 hours after application. Sections were photographed using the ×10 objective.

Published OnlineFirst December 17, 2014; DOI: 10.1158/1535-7163.MCT-13-1084

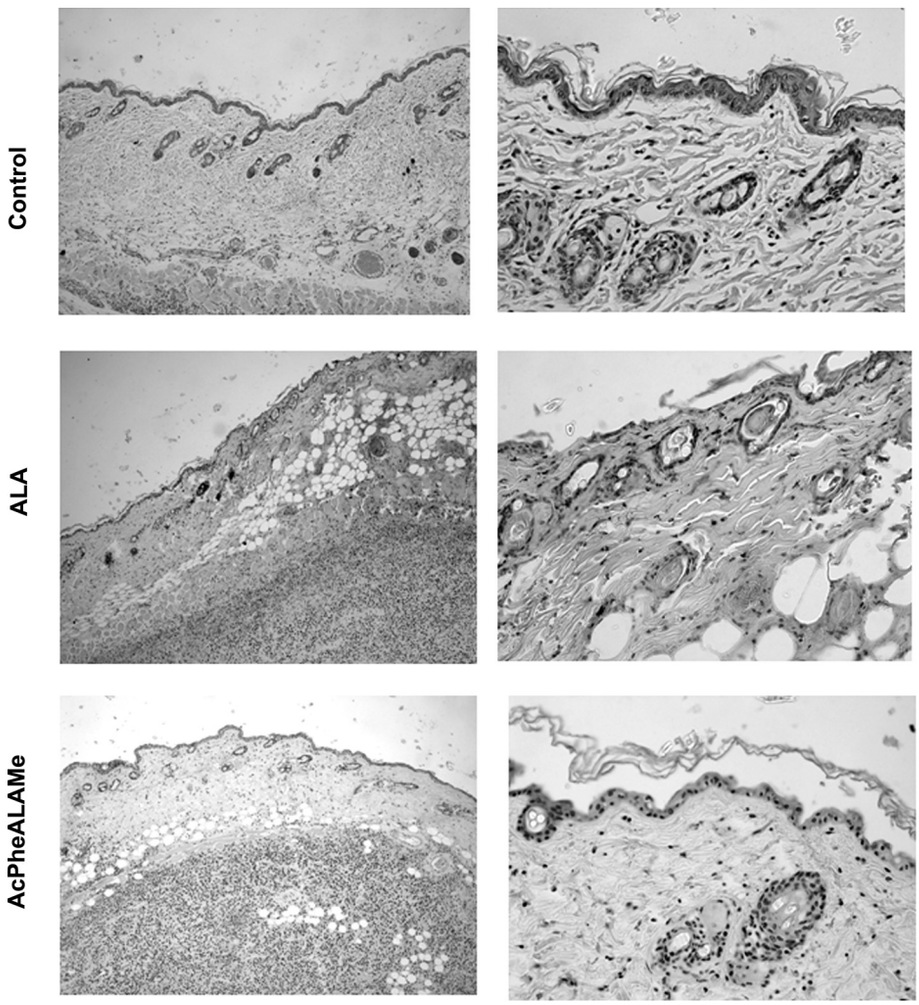

Figure 6.
Hematoxylin and eosin-stained images of SOT and adjacent tumors treated with topical ALA or Ac-Phe-ALA-Me-PDT. ALA and Ac-Phe-ALA-Me were applied topically to the SOT at dose equivalents of 3 mg ALA 3 hours before illumination. Treated SOT + tumors were excised 24 hours after the end of illumination. Sections were photographed using the ×10 (left) and ×40 (right) objective. Controls, mice illuminated without previous prodrug application.

In our *in vitro* studies, the ALA derivatives did indeed prove to be more effective than ALA in PDT treatment, inducing the same porphyrin levels but at 50 to 100-fold lower concentrations. Using a concentration of 0.01 mmol/L, the amount of porphyrins is two and three times higher for Ac-Leu-ALA-Me and Ac-Phe-ALA-Me, respectively, as compared with ALA. In addition, the performance of these peptides is even better than the best ALA ester porphryin inducer He-ALA, reaching plateau values at 5-fold lower concentrations. This improvement in porphyrin production must be due to more rapid and efficient internalization than ALA. Following illumination of cells incubated with the compounds at low concentrations (0.01 mmol/L and 3-hour exposure), LD50s were around 135 mJ/cm^2 for PAM212-Ras cells, and 45 mJ/cm^2 for PAM12 cells, whereas no cell death was induced by ALA.

In a complementary *in vivo* study using the mammary carcinoma cell line LM2, our results showed that topical application of the peptide prodrug Ac-Phe-ALA-Me is more selective than ALA, whereas systemic administration improves ALA performance, without changes on selectivity. It is worth noting that the concentrations used for both ALA peptides, that led to tumor-photosensitizing porphyrin synthesis (34) did not produce any toxic effects in mice. Through fiber-optic detection of porphyrins, we have observed that after topical application, ALA induced rapid diffusion of porphyrins to other distant sites within the skin, but this was not observed for the ALA peptides. Such a phenomenon has been previously remarked upon by us, along with a higher confinement of porphyrin synthesis from He-ALA to the application site (51). In our previous studies, a similar amount of porphyrins from ALA was synthesized in distant papillomas when compared with ALA-applied papillomas, demonstrating that either ALA itself and/or the porphyrins formed by synthesis can be distributed throughout the vasculature and accumulate in distant tumors, and though it is likely that ALA is the molecule diffusing to distant sites, we cannot discount the contribution of hydrophilic precursors of PpIX such as uroporphyrin and coproporphyrin.

On the other hand, lower porphyrin synthesis occurred in distant papillomas from He-ALA, showing that this ester and/or porphyrins formed from the precursor are more selectively localized in the site of application. Similarly, when Peng and colleagues (52) applied ALA and other ALA esters (methyl, ethyl, and propyl) to normal mouse skin, they found no porphyrins using fluorescence detection in areas other than that in which the ALA ester cream was applied, whereas in the case of ALA, a significant fluorescence was seen in the skin outside the application area. These topically applied ALA prodrugs may be retained by the

Published OnlineFirst December 17, 2014; DOI: 10.1158/1535-7163.MCT-13-1084

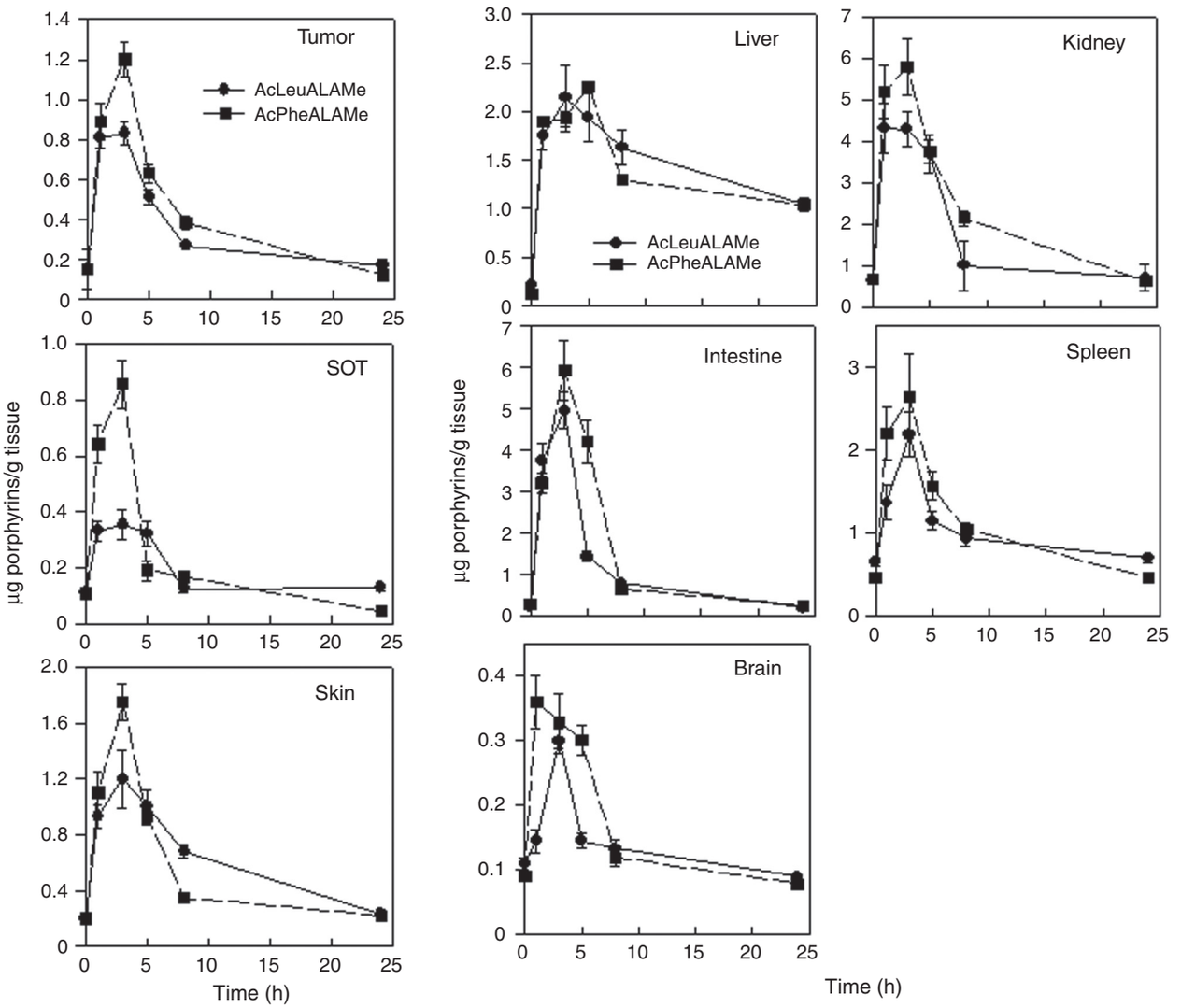

Figure 7.
Kinetics of porphyrin synthesis in tissues after Ac-Leu-ALA-Me and Ac-Phe-ALA-Me intraperitoneal (i.p.) administration. Ac-Leu-ALA-Me and Ac-Phe-ALA-Me were injected intraperitoneally at a dose equivalent of 120 mg/kg of ALA and, after different times, porphyrins were extracted from the tissues and quantified. Three mice per point were used.

stratum corneum, which may act as a reservoir (53), from which they diffuse superficially, leading to a pattern of skin porphyrin accumulation dependant on the distance from the application site.

For the novel prodrugs studied, it is possible that the ester moiety of the Ac-Phe-ALA-Me peptide is therefore responsible for the retention of the fluorescence to the site of application, with a greater extent of diffusion to the dermis as compared with ALA. In addition, the confinement to the site of application achieved by the use of ALA esters and ALA peptide esters, demonstrates that ALA, and not porphyrin, is the main molecule likely to be distributed through the bloodstream. This is supported by the tissue biodistribution and porphyrin extraction data, which demonstrate that both ALA and the ALA peptides are more specifically confined to the skin invaded by tumor (SOT) where the topical application was performed. As regards to biodistribution, Ac-Phe-ALA-Me appears to be retained less in the epidermis, but trafficks to the dermis. As has been addressed previously, the more lipophilic solutes or vehicles penetrate to a higher depth through the skin as compared with the most hydrophilic ones (54, 55). This pattern of PpIX distribution correlates to the extent of photodamage after illumination. Similar histologic changes were observed for both ALA and its phenylalanyl peptides in terms of dermal damage and depth of tumor necrosis, although epidermal damage appears to be more subtle in ALA peptide-treated SOT.

There were no differences on SOT: tumor indexes between ALA and Ac-Phe-ALA-Me; however, there was indeed a selectivity of Ac-Phe-ALA-Me for tumor and tumor skin areas with respect to distant skin, because lower distribution to distant sites through skin and tumor vasculature was obtained. This is quite relevant, because care is needed to avoid ALA-PDT–induced photosensitivity (56).

Published OnlineFirst December 17, 2014; DOI: 10.1158/1535-7163.MCT-13-1084

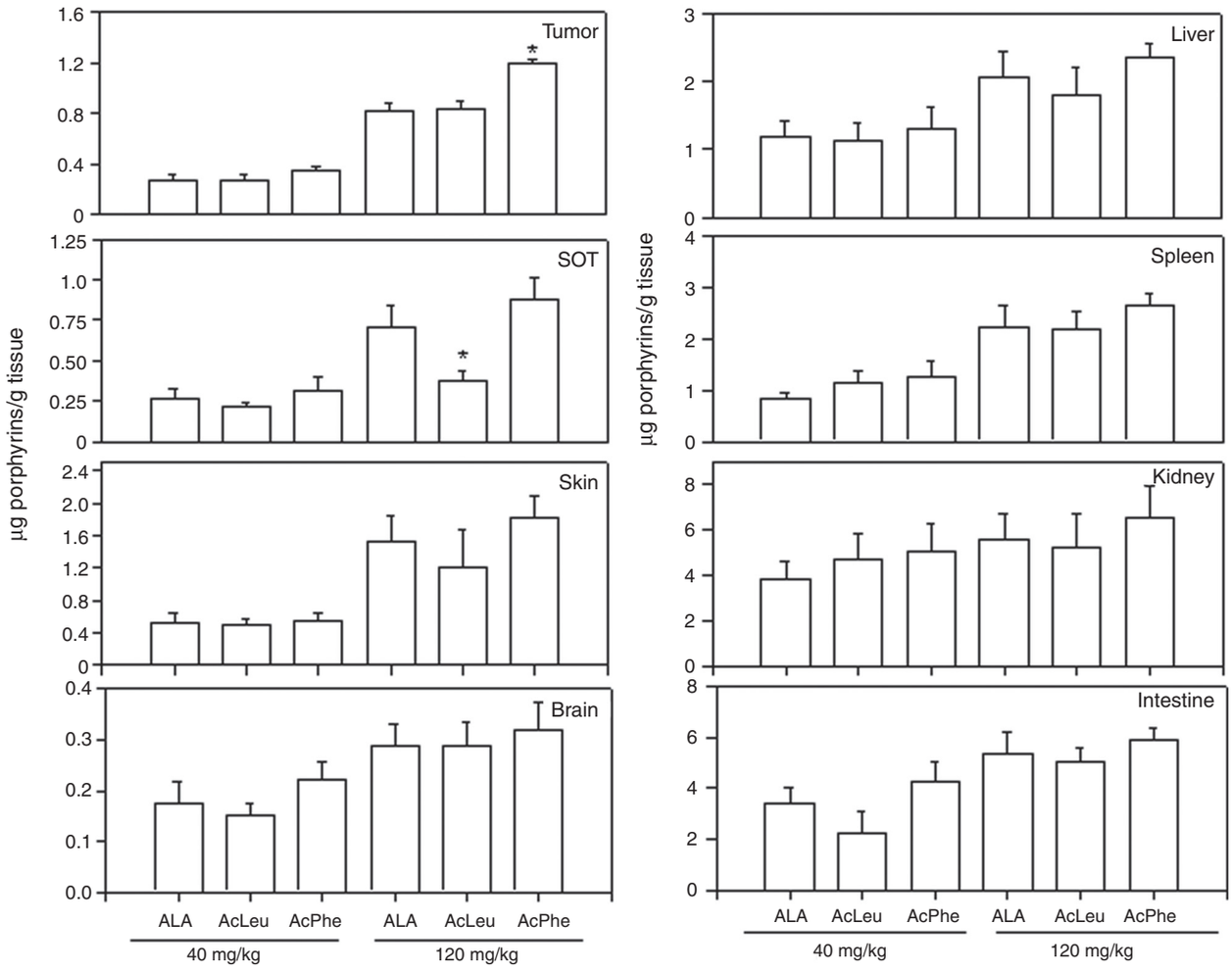

Figure 8.
Comparison of tissue synthesis from ALA and ALA peptides after systemic administration. Ac-Leu-ALA-Me and Ac-Phe-ALA-Me was injected intraperitoneally at dose equivalents of 40 and 120 mg/kg of ALA. Porphyrins were chemically extracted from tissues and determined 3 hours after injection. Three mice per point were used. *, $P < 0.05$, as compared with ALA.

The lack of any apparent toxicity, when using systemically administered ALA, is encouraging. We have also found no apparent toxicity in Wistar rats upon intravenous administration of the ALA peptides at doses of 100 mg/kg (data not shown). On the contrary, it has been reported that ALA esters containing large alkyl chains such as He-ALA cannot be administrated systemically due to their high toxicity (57). Such toxicity was ascribed by Perotti and colleagues to the ability of lipophilic esters of ALA to cross the blood–brain barrier thus inducing neurotoxicity (58). In addition, in this work, it was found that He-ALA was significantly less efficient in most tissues than ALA at producing porphyrins after intraperitoneal administration. In the present work, we have found that 3 hours after systemic administration of ALA peptides, we have obtained 1.22 ± 0.15 and 0.81 ± 0.09 µg porphyrins/g tumor tissue from Ac-Phe-ALA-Me and Ac-Leu-ALA-Me, respectively, whereas after an equivalent dose of He-ALA (58), the amount of tetrapyrroles accumulated was 0.3 ± 0.02 µg/g, a value that was slightly above basal tumor levels.

It has been previously shown that Ac-Phe-ALA-Me and Ac-Leu-ALA-Me are efficient at inducing PpIX in PAM212 cells and in pig skin explants (38, 40). N-acetyl termination appears to play an important role in metabolic processes leading to the production of PpIX from such compounds, whereas masking the C-terminus as a methyl ester does not exert a major effect (40). Using siRNA knockdown of acylaminoacyl peptide hydrolase (APEH) protein expression, we were able to show the involvement of APEH, a member of the prolyloligopeptidase family of serine peptidases, in the release of ALA from these N-acetylated peptide derivatives (39). APEH has been shown to be expressed in various normal tissues such as erythrocytes, liver, heart, testis, intestine, kidney, and brain, but its precise biologic activity is unknown (59–62). In addition, peptidase expression can be different between normal and tumor cells or tissues (63) and aminopeptidase inhibitors have been designed to target tumor cells (64–66).

In the present study, the differences between Ac-Phe-ALA-Me and Ac-Leu-ALA-Me *in vivo* may be ascribed in part to a higher ability of the former to cross biologic barriers such as skin after topical application by passive diffusion, as a function of its greater lipophilicity (clogP −0.66 vs. −1.10; ref. 38). For the case of systemic application, differential levels of peptidase activity from

Published OnlineFirst December 17, 2014; DOI: 10.1158/1535-7163.MCT-13-1084

each tissue may favor more efficient release of ALA from Ac-Phe-ALA-Me compared with Ac-Leu-ALA-Me, in tissues such as tumor, liver, skin, and kidney. The poorer performance of Ac-Leu-ALA-Me upon topical application suggests that there is an optimum lipophilicity for prodrugs of this type that is required to effectively cross a biologic barrier such as the skin. Probably the use of different vehicles could improve the performance of this derivative for PDT applications.

Although there is scarce information on the uptake mechanisms of ALA dipeptides, differential expression of proteins involved in this process may also play a role in their bioavailability *in vitro* and upon systemic administration. Several protein carriers have been identified as potential candidates for transport of ALA and its derivatives, including the dipeptide transporters PEPT1 (67) and PEPT2 (67, 68), and the amino acid carrier PAT1 (69). For instance, it is known that He-ALA interacts with PEPT1 and PEPT2 transporters (70).

In previous work, we have shown that both Ac-Phe-ALA-Me and Ac-Leu-ALA-Me penetrate PAM212 cells more easily than ALA itself (38, 40) and that ALA dipeptides entry to the cells is partly driven by passive transport, whereas He-ALA, which is more lipophilic, penetrates mainly through passive diffusion (40).

PEPT1 and PEPT2 serve as integral membrane proteins for the cellular uptake of di- and tripeptides in the organism. PEPT1 is the low-affinity, high-capacity transporter and is mainly expressed in the small intestine, whereas PEPT2 is the high-affinity, low-capacity transporter and has a broader distribution in the organism (71). Thus, we assume that PEPT2 could be relevant for ALA dipeptide uptake in tissues such as such as kidney, mammary gland, brain, or lung, whereas PEPT1 and PAT1 may be relevant to transport only in small intestine. Although PEPT1 mRNA was increased 2.3-fold in cancer tissues (69), to the best of our knowledge, there are no clear reports about overexpression of PEPT2 or PAT1 neither in tumors nor in RAS-overexpressing cell lines.

The N-terminal blocking of proteins occurs in a wide range of eukaryotic cells, where more than 50% of the cytosolic proteins can be *N*-α-acetylated. The acetylation that occurs during or after the biosynthesis of the polypeptide chains serves to protect the intracellular proteins from proteolysis. Food processing can also generate *N*-α-acetylated proteins and peptides. The mechanism underlying the intracellular catabolism of *N*-acetylated proteins has not yet been elucidated, however. It is generally assumed that two enzymes are involved in the hydrolysis of the N-terminal part of such proteins. The N-terminally acetylated peptides generated during proteolysis may be first cleaved by an APEH. This releases the N-terminal amino acid, which is in turn deacetylated by an aminoacylase (72). It is worth noting here that the amino acid residues that are usually found at the N-terminus of acetylated proteins include Ac–Met–, Ac–Ala–, and Ac–Ser– (61). This is in accordance with our previous results showing that one of our better performing ALA dipeptides was Ac–Met–ALA–Me (39).

Ac–Leu– and Ac–Phe–ALA– dipeptides are even better PpIX producers than Ac–Met–ALA–Me (39). The efficient release of ALA from Ac–Leu– and Ac–Phe–, however, appears consistent with the reported substrate and inhibitor preferences of APEH, which favors N-acetylated substrates with hydrophobic amino acid residues, and small-molecule inhibitors with aromatic substituents as side chain mimics. For example, Ac–Phe–OH was shown to induce 69% inhibition of APEH, as compared with 42% and 46% inhibition induced by its natural substrates Ac-ALA-OH and Ac-Met-OH (73), while Ac–Leu–p-nitroanilide is an efficient substrate for mammalian APEHs (74).

The main clinical application of ALA-PDT has been in the treatment of nonmelanoma skin lesions, mainly for basal cell carcinoma using topical application, although treatment of high-grade dysplasia in Barrett's esophagus, cervical neoplasia, and cancer in the oral cavity, has also been investigated (75–77). ALA administration has also been applied in the fluorescence-guided resection of bladder cancer, and intraepithelial lesions of the cervix, lung, and brain cancer (6–10). PDT can be applied to virtually any type of localized cancer that is accessible by an optical fiber, but although PDT constitutes an important therapy in dermatology, the challenge of targeting the delivery of ALA has so far hampered the translation of ALA-PDT to other oncologic applications. Our results of PpIX accumulation after intraperitoneal administration of ALA dipeptides suggest that systemically applied Ac-Phe-ALA-Me reaches every organ analyzed and particularly accumulates in tumor tissue. On the other hand, our results of topical application of ALA dipeptides highlight the ability of the phenylalanyl derivative to be confined in the area of application, cross the *stratum corneum* barrier, and reach the dermis and adjacent tumor tissue, with minimal dispersion to distant tissues. Although animal skin cancer models resembling human tumors are currently lacking, our subcutaneous implanted tumor model nonetheless provides an important first indication of the efficacy of such a derivative before translation to possible clinical applications.

In conclusion, the results in this study provide further evidence that the conjugation of ALA with specific amino acids is a promising approach for inducing enhanced intracellular porphyrin production for PDT. Our *in vivo* studies support the possibility of using particularly Ac-Phe-ALA-Me both for topical treatment of basal cell carcinomas, and also for systemic administration. Further chemical fine-tuning of this prodrug template should yield additional compounds for enhanced ALA-PDT with potential for translation to the clinic.

Disclosure of Potential Conflicts of Interest

No potential conflicts of interest were disclosed.

Authors' Contributions

Conception and design: A. Juarranz, I.M. Eggleston, A. Casas, A.J. MacRobert
Development of methodology: G. Di Venosa, P. Vallecorsa, F. Giuntini, I.M. Eggleston, A.J. MacRobert
Acquisition of data (provided animals, acquired and managed patients, provided facilities, etc.): F. Giuntini, L. Mamone, A. Batlle, S. Vanzulli, I.M. Eggleston
Analysis and interpretation of data (e.g., statistical analysis, biostatistics, computational analysis): G. Di Venosa, P. Vallecorsa, A. Juarranz, I.M. Eggleston, A. Casas, A.J. MacRobert
Writing, review, and/or revision of the manuscript: G. Di Venosa, A. Batlle, A. Juarranz, I.M. Eggleston, A.J. MacRobert
Administrative, technical, or material support (i.e., reporting or organizing data, constructing databases): A. Batlle
Study supervision: A. Juarranz, A.J. MacRobert, I.M. Eggleston

Grant Support

This work was supported by the CONICET, the Science and Technology Argentine Agency PICT 2010-0772, PICT 2008-0047 and CONICET PIP N° 11220100100173, and the BBSRC (BBD0127831 and BBD0113291; to I.M. Eggleston and A.J. MacRobert).

Received December 19, 2013; revised October 29, 2014; accepted November 19, 2014; published OnlineFirst December 17, 2014.

References

1. Dougherty T. Photodynamic Therapy-new approaches. Semin Surg Oncol 1989;5:6–16.
2. Anand S, Ortel BJ, Pereira SP, Hasan T, Maytin EV. Biomodulatory approaches to photodynamic therapy for solid tumors. Cancer Lett 2012; 326:8–16.
3. Shirasu N, Nam SO, Kuroki M. Tumor-targeted photodynamic therapy. Anticancer Res 2013;33:2823–31.
4. Brown SB, Brown EA, Walker I. The present and future role of photodynamic therapy in cancer treatment. Lancet Oncol 2004;5:497–508.
5. Fukuda H, Paredes S, Batlle A. Tumour-localizing properties of porphyrins. *In vivo* studies using free and liposome encapsulated aminolevulinic acid. Comp. Biochem Physiol 1992;102B:433–6.
6. Kennedy J, Marcus S, Pottier R. Photodynamic therapy and photodiagnosis using endogenous photosensitization induced by 5-aminolevulinic acid: mechanisms and clinical results. J Clin Laser Med Surg 1996;14:289–304.
7. Dindyal S, Nitkunan T, Bunce CJ. The economic benefit of photodynamic diagnosis in non-muscle invasive bladder cancer. Photodiagnosis Photodyn Ther 2008;5:153–8.
8. Guyon L, Ascencio M, Collinet P, Mordon S. Photodiagnosis and photodynamic therapy of peritoneal metastasis of ovarian cancer. Photodiagnosis Photodyn Ther 2012;9:16–31.
9. Nokes B, Apel M, Jones C, Brown G, Lang JE. Aminolevulinic acid (ALA): photodynamic detection and potential therapeutic applications. J Surg Res 2013;181:262–71.
10. Stummer W, Pitchimeier U, Meinel T, Wiestler OD, Zanella F, Reulen HJ. Fluorescence-guided surgery with 5-aminolevulinic acid for resection of malignant glioma: a randomized controlled multicentre phase III trial. Lancet Oncol 2006;7:392–401.
11. Harris F, Pierpoint L. Photodynamic therapy based on 5-aminolevulinic acid and its use as an antimicrobial agent. Med Res Rev 2012;32:1292–327.
12. Calzavara-Pinton P, Rossi MT, Sala R, Venturini M. Photodynamic antifungal chemotherapy. Photochem Photobiol 2012;88:512–22.
13. Peng Q, Warloe T, Moan J, Heyerdahl H, Steen HB, Nesland JM, et al. Distribution of 5-aminolevulinic acid-induced porphyrins in nodululoulcerative basal cell carcinoma. Photochem Photobiol 1995;62: 906–13.
14. Di Venosa G, Fukuda H, Batlle A, Macrobert A, Casas A. Photodynamic therapy: regulation of porphyrin synthesis and hydrolysis from ALA esters. J Photochem Photobiol B 2006;83:129–36.
15. Robinson D J, de Bruijn H S, van der Veen N, Stringer M R, Brown S B, Star W M. Fluorescence photobleaching of ALA- induced Protoporphyrin IX during photodynamic therapy of normal hairless mouse skin: the effect of light dose and irradiance and the resulting biological effect. Photochem Photobiol 1998;67:140–9.
16. Casas A, Batlle A. Aminolevulinic acid derivatives and liposome delivery as strategies for improving 5-aminolevulinic acid-mediated photodynamic therapy. Curr Med Chem 2006;13:1157–68.
17. Kloek J, Beijersbergen van Henegouwen G. Prodrugs of 5-aminolevulinic acid for photodynamic therapy. Photochem Photobiol 1996;64: 994–1000.
18. Gaullier J, Berg K, Peng Q, Anholt H, Selbo P, Ma L. Use of 5-aminolevulinic acid esters to improve photodynamic therapy on cells in culture. Cancer Res 1997;57:1481–6.
19. Perotti C, Fukuda H, Di Venosa G, MacRobert A, Batlle A, Casas A. Porphyrin synthesis from ALA derivatives for photodynamic therapy. *In vitro* and *in vivo* studies. Br J Cancer 2004;90:1660–5.
20. Vallinayagam R, Schmitt F, Barge J, Wagnieres G, Wenger V, Neier R, et al. Glycoside esters of 5-aminolevulinic acid for photodynamic therapy of cancer. Bioconjug Chem 2008;19:821–39.
21. Fotinos N, Mikulic J, Convert M, Campo MA, Piffaretti JC, Gurny R , et al. 5-ALA derivative-mediated photoinactivation of Propionibacterium acnes. J Dermatol Sci 2009;56:214–6.
22. Lee Y, Baron ED. Photodynamic therapy: current evidence and applications in dermatology. Semin Cutan Med Surg 2011;30:199–209.
23. Calzavara-Pinton PG, Venturini M, Sala R. Photodynamic therapy: update 2006. Part 2: clinical results. J Eur Acad Dermatol Venereol 2007;21: 439–51.
24. Stepp H, Waidelich R. Fluorescence diagnosis and photodynamic therapy in urology. Aktuelle Urol 2007;38:455–64.
25. Bech O, Phillips D, Moan J, MacRobert AJ. A hydroxypyridinone (CP94) enhances protoporphyrin IX formation in 5-aminolaevulinic acid treated cells. J Photochem Photobiol B 1997;41:136–44.
26. Curnow A, Pye A. Biochemical manipulation via iron chelation to enhance porphyrin production from porphyrin precursors. J Environ Pathol Toxicol Oncol 2007;26:89–103.
27. Valdés PA, Samkoe K, O'Hara JA, Roberts DW, Paulsen KD, Pogue BW. Deferoxamine iron chelation increases delta-aminolevulinic acid induced protoporphyrin IX in xenograft glioma model. Photochem Photobiol 2010;86:471–5.
28. Inoue K, Fukuhara H, Kurabayashi A, Furihata M, Tsuda M, Nagakawa K , et al. Photodynamic therapy involves an antiangiogenic mechanism and is enhanced by ferrochelatase inhibitor in urothelial carcinoma. Cancer Sci 2013;104:765–72.
29. Sinha AK, Anand S, Ortel BJ, Chang Y, Mai Z, Hasan T , et al. Methotrexate used in combination with aminolaevulinic acid for photodynamic killing of prostate cancer cells. Br J Cancer 2006;95:485–95.
30. Battah SH, Chee CE, Nakanishi H, Gerscher S, MacRobert AJ, Edwards C. Synthesis and biological studies of 5-aminolevulinic acid-containing dendrimers for photodynamic therapy. Bioconjug Chem 2001;12:980–8.
31. Battah S, O'Neill S, Edwards C, Balaratnam S, Dobbin P, MacRobert AJ. Enhanced porphyrin accumulation using dendritic derivatives of 5-aminolaevulinic acid for photodynamic therapy: an *in vitro* study. Int J Biochem Cell Biol 2006;38:1382–92.
32. Di Venosa GM, Casas AG, Battah S, Dobbin P, Fukuda H, Macrobert AJ , et al. Investigation of a novel dendritic derivative of 5-aminolaevulinic acid for photodynamic therapy. Int J Biochem Cell Biol 2006;38:82–91.
33. Casas A, Battah S, Di Venosa G, Dobbin P, Rodriguez L, Fukuda H , et al. Sustained and efficient porphyrin generation *in vivo* using dendrimer conjugates of 5-ALA for photodynamic therapy. J Control Release 2009;135:136–43.
34. Casas A, Fukuda H, Meiss R, Batlle AM. Topical and intratumoral photodynamic therapy with 5-aminolevulinic acid in a subcutaneous murine mammary adenocarcinoma. Cancer Lett 1999;41:29–38.
35. Berger Y, Greppi A, Siri O, Neier R, Jullierat-Jeanneret L. Ethylene glycol and amino acid derivatives of 5-aminolevulinic acid as new photosensitizing precursors of Protoporphyrin IX. J Med Chem 2000;43:4738–46.
36. Berger Y, Ingrassia L, Neier R, Juillerat-Jeanneret L. Evaluation of dipeptide-derivatives of 5-aminolevulinic acid as precursors for photosensitizers in photodynamic therapy. Bioorg Med Chem 2003;11:1343–51.
37. Rogers LM, McGivern PG, Butler AR, MacRobert AJ, Eggleston IM. An efficient synthesis of 5-aminolaevulinic acid (ALA)-containing peptides for use in photodynamic therapy. Tetrahedron 2005;61:6951–8.
38. Giuntini F, Bourré L, MacRobert AJ, Wilson M, Eggleston IM. Improved peptide prodrugs of 5-ALA for PDT: rationalization of cellular accumulation and protoporphyrin IX production by direct determination of cellular prodrug uptake and prodrug metabolization. J Med Chem 2009;52: 4026–37
39. Bourré L, Giuntini F, Eggleston IM, Wilson M, MacRobert AJ. Protoporphyrin IX enhancement by 5-aminolaevulinic acid peptide derivatives and the effect of RNA silencing on intracellular metabolism. Br J Cancer 2009;100:723–31.
40. Bourré L, Giuntini F, Eggleston IM, Wilson M, MacRobert AJ. 5-Aminolaevulinic acid peptide prodrugs enhance photosensitization for photodynamic therapy. Mol Cancer Ther 2008;7:1720–9.
41. Takeya H. Preparation of 5-aminolevulinic acid alkyl eters as herbicides. Chem Abs 1992;116:189633 m.
42. Yuspa SH, Hawley-Nelson P, Koehler B, Stanley JR. A survey of transformation markers in differentiating epidermal cell lines in culture. Cancer Res 1980;40:4694–703.
43. Espada J, Galaz S, Sanz-Rodríguez F, Blázquez-Castro A, Stockert JC, Bagazgoitia L , et al. Oncogenic H-Ras and PI3K signaling can inhibit E-cadherin-dependent apoptosis and promote cell survival after photodynamic therapy in mouse keratinocytes. J Cell Physiol 2009;219: 84–93.
44. Denizot F, Lang R. Rapid colorimetric assay for cell growth and survival. Modifications to the tetrazolium dye procedure giving improved sensitivity and reliability. J Immunol Methods 1986;89:271–7.
45. Workman P, Aboagye EO, Balkwill F, Balmain A, Bruder G, Chaplin DJ , et al. Committee of the national cancer research institute. Guidelines for the

welfare and use of animals in cancer research. Br J Cancer 2010;102: 1555–77.
46. Van den Akker J, Iani V, Star W, Sterenborg H, Moan J. Topical application of 5-aminolevulinic acid hexyl ester and 5-aminolevulinic acid to normal nude mouse skin: differences in protoporphyrin IX fluorescence kinetics and the role of the stratum corneum. Photochem Photobiol 2000;72: 681–9.
47. Casas A, Batlle A, Butler AR, Robertson D, Brown EH, MacRobert A, et al. Comparative effect of ALA derivatives on protoporphyrin IX production in human and rat skin organ cultures. Br J Cancer 1999;80:1525–32.
48. Rodriguez L, Di Venosa G, Batlle A, Macrobert A, Casas A. Response to ALA-based PDT in an immortalised normal breast cell line and its counterpart transformed with the Ras oncogene. Photochem Photobiol Sci 2007;6: 1306–10.
49. Bos J. Ras oncogenes in human cancer: a review. Cancer Res 1989;49: 4682–9.
50. Rodriguez-Viciana P, Tetsu O, Oda K, Okada J, Rauen K, McCormick F, et al. Cancer targets in the ras pathway. Cold Spring Harb Symp Quant Biol 2005;70:461–7.
51. Casas A, Perotti C, Fukuda H, Rogers L, Butler AR, Batlle A. ALA and ALA hexyl ester-induced porphyrin synthesis in chemically induced skin tumours: the role of different vehicles on improving photosensitization. Br J Cancer 2001;85:1794–800.
52. Peng Q, Moan J, Warloe T, Iani V, Steen HB, Bjùrseth A, et al. Build-up of esterified aminolevulinic-acid-derivative-induced porphyrin fluorescence in normal mouse skin. J Photochem Photobiol B 1996;34:95–6.
53. Rougier A, Lotte C. Correlations between horny layer concentration and percutaneous absorption. In: Shroot B, Schaeger H, editor.Pharmacology and skin: 1. Switzerland: Skin Pharmacokinetics. s; 1986.
54. Singh P. Percutaneous penetration as a method of delivery to skin and underlying tissues. In: Bronaugh R, Maibach H, editors. Percutaneous absorption: drugs-cosmetics-mechanisms-methodology. New York: Marcel Dekker; 1999. p. 597–614.
55. Dokka S, Cooper SR, Kelly S, Hardee GE, Karras JG. Dermal delivery of topically applied oligonucleotides via follicular transport in mouse skin. J Invest Dermatol 2005;124:971–5.
56. Juzenas P, Juzeniene A. Reduction of cutaneous photosensitivity by application of ointment containing ferrous or cobaltous ions concomitant with the use of topical protoporphyrin IX precursors. Photodiagnosis Photodyn Ther 2010;7:152–7.
57. Gudgin Dickinson E, Kennedy J, Pottier R. Photodynamic therapy using 5-aminolevulinic acid- induced protoporphyrin IX. In: Patrice T, editor. Photodynamic Therapy. Cambridge: The Royal Society for Chemistry; 2003. p. 81–104.
58. Perotti C, Casas A, Fukuda H, Sacca P, Batlle A. ALA and ALA hexyl ester induction of porphyrins after their systemic administration to tumour bearing mice. Br J Cancer 2002;87:790–5.
59. Yamin R, Bagchi S, Hildebrant R, Scaloni A, Widom RL, Abraham CR. Acyl peptide hydrolase, a serine proteinase isolated from conditioned medium of neuroblastoma cells, degrades the amyloid-beta peptide. J Neurochem 2007;100:458–67.
60. Erlandsson R, Boldog F, Persson B, Zabarovsky ER, Allikmets RL, Sümegi J , et al. The gene from the short arm of chromosome 3, at D3F15S2,frequently deleted in renal cell carcinoma, encodes acylpeptide hydrolase. Oncogene 1991;6:1293–5.
61. Kobayashi K, Smith JA. Acyl-peptide hydrolase from rat liver characterization of enzyme reaction. J Biol Chem 1987;262:11435–45.
62. Fujino T, Tada T, Hosaka T, Beppu M, Kikugawa K. Presence of oxidized protein hydrolase in human cell lines, rat tissues, and human/rat plasma. J Biochem 2000;127:307–13.
63. Schoenberger OL, Schwöbel H, Ebert W. N-acetylalanine aminopeptidase activity in normal and tumour cells. J Clin Chem Clin Biochem 1986; 24:375–8.
64. Aozuka Y, Koizumi K, Saitoh Y, Ueda Y, Sakurai H, Saiki I. Anti-tumor angiogenesis effect of aminopeptidase inhibitor bestatin against B16-BL6 melanoma cells orthotopically implanted into syngeneic mice. Cancer Lett 2004;216:35–42
65. Mauriz JL, Martín-Renedo J, García-Palomo A, Tuñón MJ, González-Gallego J. Methionine aminopeptidases as potential targets for treatment of gastrointestinal cancers and other tumours. Curr Drug Targets 2010; 11:1439–57.
66. Mucha A, Drag M, Dalton JP, Kafarski P. Metallo-aminopeptidase inhibitors. Biochimie 2010;92:1509–29.
67. Döring F, Walter J, Will J, Föcking M, Boll M, Amasheh S, et al. Delta-aminolevulinic acid transport by intestinal and renal peptide transporters and its physiological and clinical implications. J Clin Invest 1998. 101:2761–7.
68. Kamal MA, Keep RF, Smith DE. Role and relevance of PEPT2 in drug disposition, dynamics, and toxicity. Drug Metab Pharmacokinet 2008;23: 236–42.
69. Anderson CM, Jevons M, Thangaraju M, Edwards N, Conlon NJ, Woods S, et al. Transport of the photodynamic therapy agent 5-aminolevulinic acid by distinct H+-coupled nutrient carriers coexpressed in the small intestine. JPharmacol Exp Ther 2010;332:220–8.
70. Rodriguez L, Batlle A, Di Venosa G, MacRobert AJ, Battah S, Daniel H, et al. Study of the mechanisms of uptake of 5-aminolevulinic acid derivatives by PEPT1 and PEPT2 transporters as a tool to improve photodynamic therapy of tumours. Int J Biochem Cell Biol 2006;38:1530–9.
71. Rubio-Aliaga I, Daniel H. Peptide transporters and their roles in physiological processes and drug disposition. Xenobiotica 2008;38:1022–42.
72. Perrier J, Durand A, Giardina T, Puigserver A. Catabolism of intracellular N-terminal acetylated proteins: involvement of acylpeptide hydrolase and acylase. Biochimie 2005;87:673–85.
73. Driessen HP, de Jong WW, Tesser GI, Bloemendal H. The mechanism of N-terminal acetylation of proteins. CRC Crit Rev Biochem 1985;18:281–325.
74. Palmieri G, Bergamo P, Luini A, Ruvo M, Gogliettino M, Langella E , et al. Acylpeptide hydrolase inhibition as targeted strategy to induce proteasomal down-regulation. PLoS ONE 2011;6:e25888.
75. Pech O, Gossner L, May A, Rabenstein T, Vieth M, Stolte M, et al. Long-term results of photodynamic therapy with 5-aminolevulinic acid for superficial Barrett's cancer and high grade intraepithelial neoplasia. Gastrointest Endosc 2005;62:24–30.
76. Mallia RJ, Subhash N, Sebastian P, Kumar R, Thomas SS, Mathews A, et al. *In vivo* temporal evolution of ALA-induced normalized fluorescence at different anatomical locations of oral cavity: application to improve cancer diagnostic contrast and potential. Photodiagnosis Photodyn Ther 2010;7:162–75.
77. Barnett AA, Haller JC, Cairnduff F, Lane G, Brown SB, Roberts DJ. A randomised, double-blind, placebo-controlled trial of photodynamic therapy using 5-aminolaevulinic acid for the treatment of cervical intraepithelial neoplasia. Int J Cancer 2003;103:829–32.

Published OnlineFirst December 17, 2014; DOI: 10.1158/1535-7163.MCT-13-1084

Molecular Cancer Therapeutics

The Use of Dipeptide Derivatives of 5-Aminolaevulinic Acid Promotes Their Entry to Tumor Cells and Improves Tumor Selectivity of Photodynamic Therapy

Gabriela Di Venosa, Pablo Vallecorsa, Francesca Giuntini, et al.

Mol Cancer Ther 2015;14:440-451. Published OnlineFirst December 17, 2014.